Journal of Power Sources 201 (2012) 360–367

Contents lists available at SciVerse ScienceDirect

Journal of Power Sources

journal homepage: www.elsevier.com/locate/jpowsour

An insight into the electrochemical behavior of Co/Al layered double hydroxide thin films prepared by electrodeposition

Erika Scavetta[a,*], Barbara Ballarin[a], Claudio Corticelli[a], Isacco Gualandi[a], Domenica Tonelli[a], Vanessa Prevot[b,c], Claude Forano[b,c], Christine Mousty[b,c,**]

[a] Dip. Chimica Fisica e Inorganica, ALMA MATER STUDIORUM-Università di Bologna Viale Risorgimento 4, 40136 Bologna, Italy
[b] Clermont Université, Université Blaise Pascal, Laboratoire des Matériaux Inorganiques, BP 10448, F-63000 Clermont-Ferrand, France
[c] CNRS, UMR 6002, LMI, F-63177 Aubière, France

ARTICLE INFO

Article history:
Received 5 September 2011
Accepted 31 October 2011
Available online 6 November 2011

Keywords:
Co/Al layered double hydroxide
Electrodeposition
Coated electrode
Electrooxidation

ABSTRACT

A detailed study aimed at clarifying the electrochemical behavior of Co/Al-LDH thin films, prepared on Pt electrode by electrodeposition at −0.9 V, has been carried out. Reproducible thin and homogeneous films with variable amounts of LDH coated on the electrode surface have been achieved by varying the electrodeposition time (t = 5, 10, 30 and 60 s): 29.2 ± 0.7, 37.9 ± 1.4, 55.1 ± 2.1 and 62.5 ± 4.3 μg cm^{-2}, respectively. X-ray diffraction, spectroscopic techniques and the electrochemical quartz crystal microbalance analysis have been used to give an insight into the phase changes occurring when the as-prepared Co/Al-LDH thin films were oxidized and reduced by cycling the potential between 0 and 0.6 V/SCE in 0.1 M KOH. Our experiments demonstrate that the irreversible oxidation peak observed in the first cycle corresponds to the transformation of the Co(II)/Al-LDH phase in a γ-Co(III)OOH like phase. This resulting phase is stable under cycling and shows a pseudo-capacitive behavior with an estimated specific capacitance of 500 F g^{-1}.

1. Introduction

Layered double hydroxides (LDH) or hydrotalcite-like compounds (HTlc) are lamellar compounds with the chemical formula $[M_a(II)_{1-x}M_b(III)_x(OH)_2]^{x+}(A^{n-}_{x/n}) \times mH_2O$, shortly named M_a/M_b-A, where M_a(II) and M_b(III) are metal cations, A^{n-} is an anion. Pure LDH phases with M_a equal cobalt can be obtained with x ranging between 0.22 and 0.50 [1,2]. Due to their anion exchange and intercalation properties and their wide range of metal compositions, LDH have found many applications in different fields, such as precursors for coatings and catalysts [3,4], hosts for photoactivation and photocatalysis [5] and anion exchangers [6]. More recently, these materials have been also applied with increasing interest to the electrochemical field, in energy storage devices [7,8], as electrode coatings for amperometric or potentiometric sensors [9–11] and as biosensors, being suitable hosts for enzymes [12,13]. In particular, cobalt containing LDH phases have been evaluated as amperometric sensors to detect sugars [14]. Recently, an electrochromic device, based on an ITO electrode coated with a thin film of electrodeposited Co/Al-LDH, has been successfully developed [15]. Furthermore, Co based LDH modified electrodes, as thin films or as pressed electrodes, have been used as supercapacitors, energy storage devices that possess high energy densities and long cycle lifetimes [16–23].

Note that Co containing LDH phases can be easily prepared by coprecipitation involving the mixing of a metal salt solution and an alkaline solution [24]. However with the aim of tuning structural and morphological properties of LDH, alternative synthetic methods have been described. Uniform and large-sized platelets of well-crystallized Co/Al-LDH have been synthesized by homogenous precipitation method based on the slow hydrolysis of urea [25]. Recently, O'Hare *et al.* [26] reported that the combination of homogenous precipitation and reverse microemulsion method permits to prepare Co/Al-LDH nanoplatelets with controlled particle sizes. Co based LDH gels are also accessible either by a sol–gel process involving hydrolysis and condensation of alkoxides precursors in alcohol [27,28] or by acetate precursors hydrolysis in polyol medium [29].

Moreover, to prepare LDH thin films, a promising procedure optimized in the last few years by Scavetta *et al.* [30,31] consists of a one-step electrodeposition of Ni/Al or Co/Al-LDHs allowing simultaneously LDH synthesis and modification of the electrode's

* Corresponding author. Tel.: +39 0512093256; fax: +39 0512093690.
** Corresponding author at: Clermont Université, Université Blaise Pascal, Laboratoire des Matériaux Inorganiques, BP 10448, F-63000 Clermont-Ferrand, France. Tel.: +33 473 407 598; fax: +33 473 407 108.
E-mail addresses: erika.scavetta2@unibo.it (E. Scavetta), Christine.Mousty@univ-bpclermont.fr (C. Mousty).

0378-7753/$ – see front matter © 2011 Elsevier B.V. All rights reserved.
doi:10.1016/j.jpowsour.2011.10.122

surface. This method is based on electrochemical generation of hydroxide anions by cathodic reduction of nitrate ions. Advantages of the proposed method are the short time needed to carry out the deposition and the possibility of modulating the electrolytic bath composition and the electrosynthesis time to tune the film thickness and the Ni/Al or Co/Al ratios [30,31]. However the electrodeposited materials display a poor crystallinity and are difficult to characterize due to the small amount of solid deposited on the electrode surface (few micrograms).

It is interesting to underline that Co/Al-LDH films display a different electrochemical behavior than Ni/Al-LDH thin films obtained using a similar synthetic process [31]. Firstly, cyclic voltammetry and spectroelectrochemistry revealed an irreversible phase transition occurring during the first anodic cycling of the coated electrode in an alkaline solution. Secondly, the stable film as-obtained is characterized by two distinct couple of peaks. Since a detailed knowledge of the active material is the starting point of all application, the present work is aimed to provide a further insight into the Co/Al-LDH behavior under redox process using structural and spectroscopic techniques, such as powder X-ray diffraction (PXRD), Infrared (FTIR) and Raman spectroscopies, with particular attention to structural changes. In addition, the electrochemical quartz crystal microbalance (EQCM) was employed to deeper study the amount of LDH deposited on the Pt electrode for the different pulse lengths and the changes of mass taking place during the electrochemical oxidation process.

2. Experimental

2.1. Chemicals

All chemicals (Fluka) were of reagent grade purity and used as received. All solutions were prepared with doubly distilled water from a glass distillation apparatus. The Co/Al-NO_3 LDH was electrosynthesized from freshly prepared solutions of cobalt and aluminum nitrates.

2.2. Apparatus

All the electrochemical experiments were carried out in a single compartment, three-electrode cell. Electrode potentials were measured with respect to an aqueous saturated calomel electrode (SCE). A Pt wire was used as the counter electrode. The CV curves were recorded using a CHInstruments Mod. 660C, controlled by a personal computer *via* CHInstruments software. An Autolab PGSTAT20 (Ecochemie, Utrecht, The Netherlands) potentiostat/galvanostat interfaced with a personal computer was used in the EQCM experiments which were performed with a MAXTEK PM-710 device.

The PXRD patterns of the powder samples and thin films were recorded using a Philips X'Pert Pro diffractometer with a Cu Kα radiation ($\lambda = 0.15415$ nm) in the 2–70° 2θ range, in steps of 0.0334° with a counting time per step of 650 s. Raman spectroscopy measurements were performed using a Jobin Yvon Horiba T64000 equipped with a liquid N_2 cooled CCD detector. An Ar laser line at 515.5 nm was used as excitation source with a power of 20 mW. Attenuated Total Reflectance-FTIR spectra were recorded on a Nicolet 5700 (Thermo Electron Corporation) spectrometer.

The chemical composition of LDH films were investigated by SEM/EDS analysis, using an EVO 50 Series Instrument (LEO ZEISS) equipped with an INCA Energy 350 EDS microanalysis system and INCA SmartMap for imaging the spatial variation of the elements in a sample (Oxford Instruments Analytical). The accelerating voltage was 25 kV or 10 kV, the beam current 1.5 nA and the spectra collection time 100 s. FEG-SEM images were acquired with a Zeiss Supra 55 FEG-VP operating at 3 keV. Atomic Force Microscopy (AFM) experiments were performed with AFM, Scanning Probe Microscope Vista 100, Burleigh Instruments Inc., equipped with a long-range 100 Å tip, operating in contact mode with a 10 nN constant force. Thermogravimetric (TG) analyses were carried out in a TGA 2050 instrument from TA instruments in flowing air, at a heating rate of 10 °C min^{-1} from 30 to 1000 °C.

2.3. Preparation of modified electrodes

Pt electrodes were polished to a mirror-like surface with an aqueous alumina (Logitech) slurry of three different granulometries (1, 0.3 and 0.05 μm) on a wet polishing cloth, rinsed with distilled water and then sonically cleaned in a 1:1 ethanol/water mixture, for 10 min, to remove any trace of alumina. The bare electrode was dried at room temperature after rinsing with carbon dioxide-free water. The films of Co/Al-NO_3 LDH were deposited on the electrode surface by cathodic reduction of a 0.03 M metal cation solution containing $Co(NO_3)_2$ and $Al(NO_3)_3$ with a Co/Al molar ratio 3/1 and 0.3 M KNO_3. The electrochemical reaction was carried out in a single compartment three-electrode cell, by applying a potential of −0.9 V *vs* SCE for a deposition time (t) of 5, 10, 30 or 60 s [31]. After electrodeposition, the films were rinsed gently with doubly distilled water, dried in a dessiccator over silica gel and then promptly submitted to the various characterization analyses. For the EQCM tests the electrosynthesis was carried out on 5 MHz-AT cut quartz crystal coated with sputtered Pt (surface area 1.37 cm^2). Solid state characterizations (PXRD and spectroscopic analysis) were performed either on a platinum plate of 1 cm^2 or on powders collected from Pt substrate after electrodeposition repeated 10 times for an electrolysis time of 60 s.

3. Results

3.1. Deposition of Co/Al-LDH films by electrosynthesis

Co/Al-LDH was deposited at a Pt electrode surface by cathodic reduction of aqueous solution of nitrates ($NO_3^- + H_2O + 2e^- \rightarrow NO_2^- + 2OH^-$) at −0.9 V/SCE. The electrochemical deposition was carried out for different deposition times ($5 \leq t \leq 60$ s) and the electrodeposition process has been monitored by EQCM. Fig. 1 reports the plot of the current and the related change of mass recorded during a potential step of 60 s. In the first stages of the pulse application, there is a rapid increase of mass at the electrode (50% of the mass is overtaken after 5 s) followed by an almost linear but slower increase in mass. The shape of this curve is consistent with the mechanism previously postulated for LDH precipitation by electrosynthesis [30]: as long as the cathodic potential is applied, the pH necessary for the LDH precipitation can be reached and the coprecipitation of the Co/Al-LDH starts very rapidly. Indeed, curve c in Fig. 1 clearly shows the linear relation between the mass increase and the cathodic charge with a slope of 1 mg C^{-1}. When the mass density becomes higher than 35 μg cm^{-2}, the electrodeposition efficiency is decreased, probably due to diffusional constraints of the reactive species (NO_3^-, OH^-, Co^{2+}, Al^{3+}) throughout the Co/Al-LDH coating. This electrodeposition process has been repeated five times for each deposition time, with the aim of investigating the repeatability. The amounts of deposited LDH were 29.2 + 0.7, 37.9 ± 1.4, 55.1 ± 2.1 and 62.5 ± 4.3 μg cm^{-2} for 5, 10, 30 and 60 s deposition times, respectively. The repeatability of the LDH deposition increases as the deposition time decreases since the LDH coating is much thinner and more homogeneously distributed on the electrode surface.

The as-prepared Co/Al-LDH thin film (t = 60 s) was characterized by FEG-SEM and AFM analyses to gain information on its

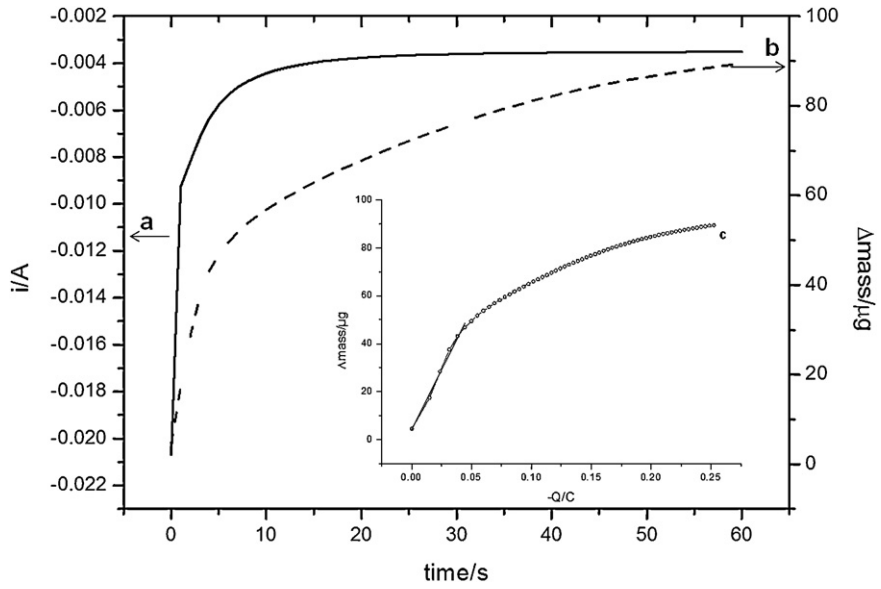

Fig. 1. Variation of current (curve a) and mass (curve b) recorded by the EQCM during the Co/Al-LDH electrodeposition. Variation of mass as a function of the cathodic charge (curve c) ($E_{appl} = -0.9$ V; $t = 60$ s).

morphology (Fig. 2). The film thickness was estimated by AFM at 300 ± 14 nm [31]. The FEG-SEM and AFM images reveal a dense and homogeneous film characterized by a relatively rough surface due to the presence of pseudo-sperical particles whose dimensions range from 100 nm to about 300 nm (Fig. 2, inset). As previously observed for Ni/Al-LDH thin film electrodeposition, ill-defined LDH particles with a random orientation are produced during the *in situ* electrodeposition at the surface of the electrode. No preferential orientation of the LDH platelets can be distinguished here, in contrast to the perpendicular or parallel orientation of LDH platelets observed in the case of thin LDH films prepared by *in situ* growth using urea or ammonia as precipitant agent [22].

EDS analysis was also performed on the same film to study the elemental composition of the deposited material. In particular the Co/Al ratio, a key parameter in LDH-like materials which determines many of their physico-chemical properties, has been investigated. Furthermore, the potassium content in the films has also been determined since a previous work demonstrated it was present in abundance, and homogeneously distributed on LDH-modified electrodes after electrosynthesis [32]. The analysis was

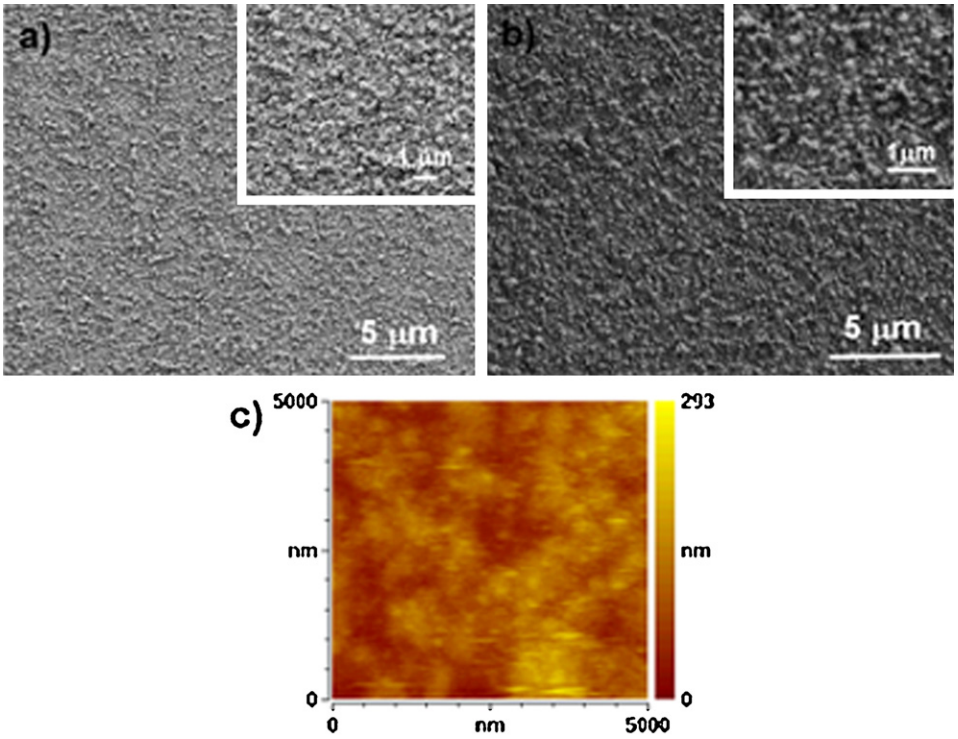

Fig. 2. FEG-SEM images of the Co/Al-LDH films deposited on the Pt electrode for 60 s (a) before and (b) after potential scan (in inset high magnification FEG-SEM images) and (c) AFM image of the as-prepared film before (or after) potential scan.

Table 1
EDS analysis of Co/Al-LDH.

Accelerating voltage (kV)	Cobalt atomic (%)	Aluminum atomic (%)	Potassium atomic (%)	Platinum atomic (%)	Co/Al atomic ratio	K/Co atomic ratio
10	10.8	4.2	5.1	7.6	2.5	0.5
25	5.0	2.0	4.8	9.7	2.5	1.0

performed at two different accelerating voltages (25 kV and 10 kV) in order to have a different penetration width and therefore to gain some information on the film composition along the perpendicular direction to the surface. From the EDS data (Table 1) we can argue that the Co/Al-LDH material grown on the Pt electrode surface has always the same composition (Co/Al ratio = 2.5) in agreement with the hypothesis that the LDH precipitation proceeds in a single step without the preliminary precipitation of the aluminum hydroxide phase. Consequently local high OH^- supersaturation and pH value must arise at the surface of the Pt electrode forcing Co(II) and Al(III) to precipitate together. Potassium is always present in a high amount and the EDS data show that it is not just adsorbed on the surface of the LDH but even more conspicuous amount of potassium is contained in the inner layers. To further corroborate this statement EDS analysis was again performed after washing several times the electrode with double distilled water. Yet, the percentages of the different elements were unchanged. This could be explained hypothesising that some K^+ ions are adsorbed and trapped on the electrode surface during the cathodic polarisation.

PXRD analysis was performed in order to identify the structure of the various electrodeposited thin films. PXRD patterns (Fig. 3A, curve a), after baseline correction, is typical of a Co/Al-LDH structure with a low crystallinity as mentioned in our previous works for electrodeposited LDH thin films [30,31,33]. All reflections can be indexed as those typical of a hydrotalcite-like structure (JCPDS: 38-0487). In particular, the reflections at 8.29, 4.11, 2.66 and 1.53 Å correspond to diffraction by the 003, 006, 012 and 110 basal planes, respectively, and are compatible with a nitrate containing LDH structure (Table 2). Note that additional diffraction lines (23.60, 29.45, 33.66, 41.19, and 46.30 Å) are also observed on the PXRD pattern which can be assigned, respectively to the 111, 012, 130, 220, and 113 diffracting planes of orthorhombic KNO_3. The presence of crystallized KNO_3 into the electrodeposited films, in agreement with the results obtained by EDS, indicates that KNO_3 is trapped in the pores of the films and crystallized under drying.

FTIR and Raman spectra of the film (Fig. 4A, curve a and B, curve a) confirm the formation of the Co/Al-NO_3 LDH phase. The broad and intense bands in the 3200–3700 cm^{-1} region (data not shown)

Table 2
XRD data of Co/Al-LDH and γ-$Co_{1-x}Al_xOOH$ phases.

	Distance values (Å)			
	003	006	012	110
Co/Al-LDH	8.21	4.10	2.62	1.53
$Co/Al\text{-}LDH_{KOH}$	7.69	3.84	2.63	1.53
γ-$Co_{1-x}Al_xOOH$	6.89	3.49	2.41	1.43
γ-CoOOH (ceramic route [38])	6.79	3.40	2.43	1.41
γ-CoOOH (soft process [39])	6.70	3.40	2.40	1.40

is due to the ν_{O-H} stretching vibrations of the layer hydroxides and intercalated water molecules. The band at 1626 cm^{-1}, corresponding to the H_2O bending mode (δ_{HOH}), is sufficiently intense to account for a highly hydrated film. The sharp bands at 1380 cm^{-1} and 826 cm^{-1} on the FTIR spectrum and at 1052 cm^{-1} and 716 cm^{-1} on the Raman spectrum are ascribable, respectively to the stretching and the bending mode of the nitrate anions arising from both intercalated LDH anions and KNO_3 phase. Below 1000 cm^{-1}, the bands corresponding to the stretching modes of the brucite-like layers are present. As previously described in the literature [34], the bands attributed to translational modes of Al-OH and Co-OH and the band ascribed to M–O–M bonds are recorded, respectively between 810–500 cm^{-1} and 427 cm^{-1} on the FTIR spectra. The low frequency region of the Raman spectra accounts for the analogous molecular vibrations. The Raman spectrum is very similar to that we reported previously for electrodeposited Ni/Al-NO_3 LDH films [33]. Substitution of Ni^{2+} by Co^{2+} in the brucite-like layers shifts the $\nu(M^{2+},Al\text{–}O)$ vibration bands to lower energy values.

The amount of adsorbed and intercalated water molecules determined by thermal analysis from the weight loss occurring at 100 °C, corresponds to 0.6H_2O molecules per total metal (Co + Al). Then, on the basis of the PXRD, FTIR and Raman spectroscopies and on quantitative analysis from EDS, we can assume the following chemical formula: $Co_{0.71}Al_{0.29}(OH)_2(NO_3)_{0.29}\cdot 0.6H_2O$. An amount of KNO_3 comprised between 0.36 and 0.71 per LDH formula unit is also present in the film.

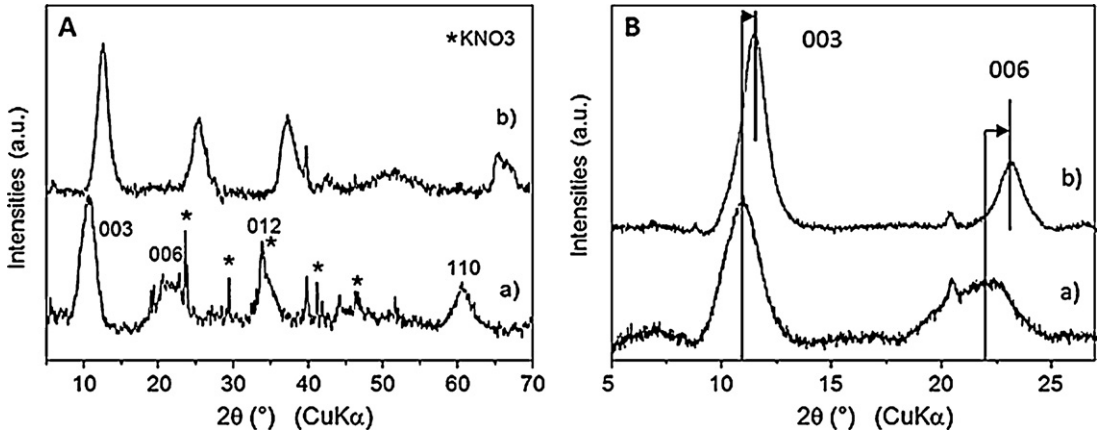

Fig. 3. (A) PXRD patterns of Co/Al-LDH powder obtained (a) after 10 different electrodepositions for 60 s, (b) after the first voltammetric cycle. (B) X-ray diffraction of Co/Al-LDH powder obtained (a) after 10 different electrodepositions for 60 s and (b) exchanged by carbonate in 0.1 M KOH.

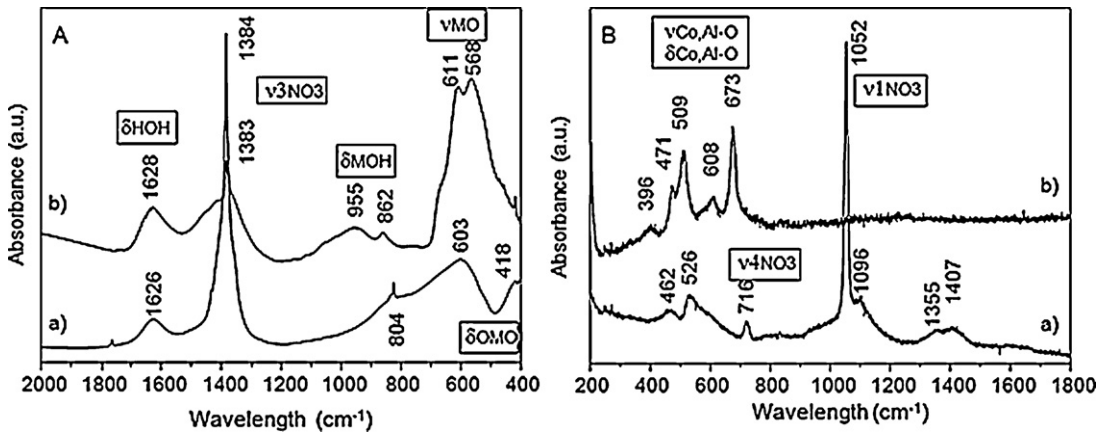

Fig. 4. (A) FTIR and (B) Raman spectra of Co/Al-LDH powder obtained (a) after 10 different electrodepositions for 60 s and (b) after the first voltammetric cycle.

3.2. Electrochemical behavior of electrodeposited Co/Al-LDH in basic solution

Co/Al-LDH is an electroactive material which can be characterized by cyclic voltammetry (CV) in basic medium (0.1 M KOH). In order to give a further insight on the phase modification occurring during the oxidation process, mass changes were recorded by EQCM coupled with CV experiments and the resulting oxidized film was characterized by PXRD, FTIR and Raman spectroscopies.

Firstly, we investigated the effect of the strong basic KOH working solution on the chemical stability of the Co/Al-LDH coated electrode (t = 60 s). To correctly estimate this effect by EQCM, and in particular in order to consider even the early dipping times, the electrode was dipped in a doubly distilled water solution and, once the recorded frequency had reached a stable value, an addition of concentrated KOH solution was made to obtain a final KOH concentration of 0.1 M. As soon as KOH is added into the solution, a sudden decrease of the mass is observed (12 μg), then the frequency becomes stable and it does not change for more than 1000 s (Fig. 5). Such a variation of mass can be ascribed, in one hand, to the complete substitution of nitrate anions with carbonate. Indeed assuming the hypothetical formula calculated above and the amount of Co/Al-LDH deposited on the electrode (85 μg), the variation of mass calculated for a total exchange of 2×10^{-7} mol of NO_3^- by 1×10^{-7} mol of CO_3^{2-} should be 7 μg. In another hand, some leaching of KNO_3 salt from the LDH thin film into KOH electrolyte solution and change in hydration state should also be considered (*vide infra*).

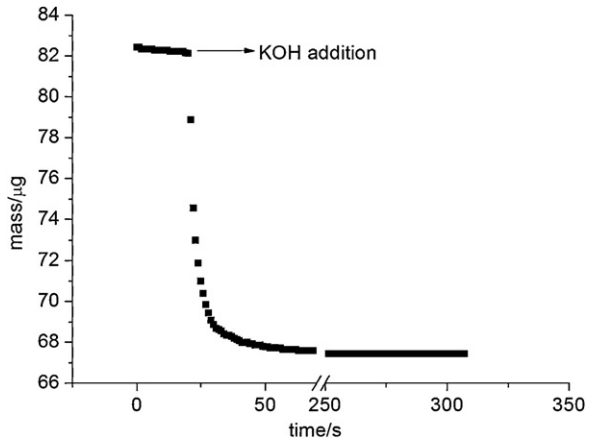

Fig. 5. Plot of the mass recorded as a function of time for a Co/Al-LDH coated electrode (t = 60 s) in a water solution after 1 M KOH addition, the final KOH concentration being 0.1 M.

The complete replacement of nitrate by carbonate anions inside the LDH structure was further confirmed by PXRD (Fig. 3B). Indeed, after dipping the electrode in KOH solution, PXRD pattern reveals an increase of the crystallinity of the material with sharper peaks, especially the $h\,k\,l$ diffractions peak characterizing the layer (Table 2). In addition, the basal spacing determined from the d_{003} and d_{006} distances shifts from 8.21 Å, typical of a LDH containing nitrate, to 7.69 Å which is typical of a carbonate containing LDH structure. Such modification of the LDH interlayer anion is explained by the stronger affinity of LDH matrix for carbonate anions than for nitrate anions. Moreover, presence of carbonate anion from atmospheric CO_2 dissolution, is due to the strong basic medium used.

Secondly, to evaluate the electrochemical behavior of Co/Al-LDH in 0.1 M KOH solution, EQCM experiments coupled with cyclic voltammetry were recorded in the potential range 0–0.6 V *vs* SCE using a thinner film, in order to improve the sensitivity of the measurement. The experiment depicted in Fig. 6 has been performed with an electrode coated with 38 μg of LDH (t = 5 s) corresponding to 3.7×10^{-7} mol.

The first scan (Fig. 6A) is dominated by an anodic irreversible peak (A) at 0.26 V which could be ascribed to the oxidation of the Co(II) cations to Co(III); the number of oxidized Co moles calculated from the integration of the oxidation peak at low scan rate ($0.01\,V\,s^{-1}$) was 1.95×10^{-7}. According to the formula proposed for the electrodeposited LDH film containing KNO_3, almost 80% of the Co(II) cations are concerned, indicating a quasi-complete oxidation of the LDH phase. This shows the quite high electrochemical accessibility of the Co cations within the LDH layer. Moreover in the first scan, we observe a broad peak of small intensity at a potential of 0.40 V (peak B) which can be ascribed to the further oxidation of a small part of the generated Co(III) species to Co(IV). Due to the highly capacitive shape of the CV response in this potential region, it is not easy to correctly consider the faradic contribution and therefore to accurately calculate the number of Co cations involved in this second electron transfer process. One can estimate that 4.2×10^{-9} mol are involved, which corresponds to only 2% of the Co(III) generated in the previous process. The reverse scan is characterized by two peaks of small intensity, the first at 0.40 V (B′) and the second at 0.15 V (C) which correspond to the reverse reduction Co(IV) → Co(III) and Co(III) → Co(II), respectively [16–18].

As to the plot of the mass is concerned, simultaneously to the oxidation at 0.26 V (peak A), the mass irreversibly decreased by 2.2 μg. The plot of the mass versus the anodic charge resulted

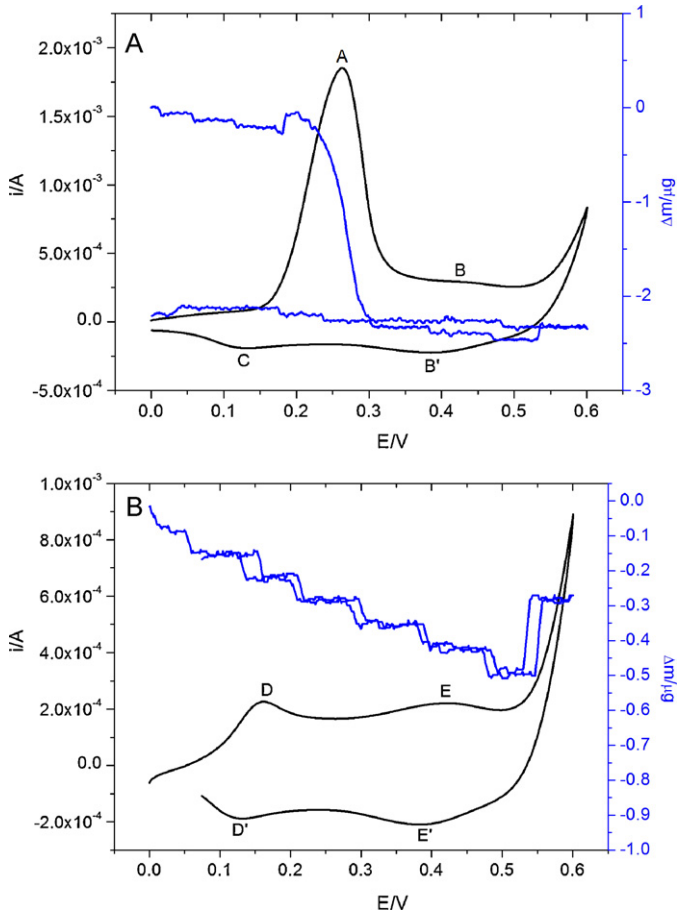

Fig. 6. Mass changes during potential scans for Co/Al-LDH coated electrode in 0.1 M KOH (A) first scan, (B) second scan. Potential scan rate: 0.01 V s^{-1}.

linear in the potential range 0.15–0.29 V with a slope of 11 g mol^{-1} being the apparent mass per mole of electrons. Similarly, Roto *et al.* observed the same highly irreversible decrease in the mass during oxidation of a Ni/Al-LDH coated electrode at high pH and explained it by the instability of the Ni/Al-LDH phase and a partial transformation of the LDH phase into a β-$Ni(OH)_2$ [35]. After this first irreversible mass drop, unlike Ni/Al-LDH coated electrodes the following scans are characterized by very small and reversible mass changes (Fig. 6B).

To get better insight on the structural modification of the Co/Al-LDH phase occurring under the potential scan the new generated phase has been characterized by PXRD and spectroscopic techniques. The structural characterization has been made on the material after one complete scan with a final potential at 0.0 V where it appears to be stable. It should be underlined that tests have been made to evaluate the stability of the oxidized material by measuring the open circuit potential (o.c.p.) of the modified electrode just at the end of the anodic scan (E = 0.60 V). However under such conditions, the material seems to be not stable, tending its o.c.p. to decrease.

The diffractogram of the thin film after one voltammetric scan is shown in Fig. 3A (curve b). Compared to the starting LDH structure, the XRD pattern of the phase obtained after potential scan reveals a deep modification. Despite the poor crystallinity of the phase, it is clearly observed that all the diffraction lines that is the basal and higher order 0 0 l reflections and the non basal $h\,k\,l$ reflection are shifted at higher 2θ values (Table 2). The 0 0 3 diffraction line characteristic of the interlayer distance shifts from 7.68 Å for the Co/Al–CO_3 phase formed in basic medium to 6.89 Å for the oxidized phase whereas the 1 1 0 reflection evolves from 1.53 Å to 1.43 Å. Such a displacement of the diffraction lines cannot be explained by a partial oxidation of the Co(II) into the layer leading to a $Co^{II}Co^{III}Al^{III}$-LDH phase associated with an anion intercalation to balance the charge in excess produces by the oxidation process. Indeed, LDH phases containing intralayer cobalt cations in two different oxidation states have previously been reported in the literature [36,37]. Yet, the partial modification of the Co oxidation state induces only a slight modification of the *a* lattice parameter, which is systematically described in the range of 1.53 ± 0.1 Å, in good agreement with a maintain of the brucite-like structure. In the present work, the XRD pattern modifications and particularly the shift of the 1 1 0 reflection clearly evidence that the first irreversible oxidation process of Co/Al-LDH precursor phase (peak A in CV), leads to the formation a new layered Co/Al-based phase which appears comparable to the γ-CoOOH-like phase reported in the literature [38,39]. This is in good agreement with the voltammetric characterization and in particular with the postulated almost complete oxidation of all the Co(II) cations. It is this new phase which is involved in the subsequent electrochemical processes (peaks B, B′ and C).

In Table 2, the distance values between reflection planes obtained from PXRD data are reported for the Co/Al-LDH precursor phases (NO_3^- and CO_3^{2-}) and the oxidized phase. For comparison, are also presented distances corresponding to a γ-CoOOH phase obtained either by ceramic route involving oxidizing hydrolysis of M_xCoO_2 (M = Na, K) precursor [38] or by soft chemistry processes [39] based on the oxidation reaction of α-$Co(OH)_2$. This modification of Co based LDH phase confirms that precursors already presenting a large interlayer domain are necessary to access to γ-CoOOH phase (also written as $HCoO_2$) as suggested by Bardé *et al.* [39]. Under electrochemical oxidation, the Co/Al-LDH phase obviously transforms in a γ-CoOOH analogous phase containing aluminum cations: γ-$Co_{1-x}Al_xOOH$. Considering that Co/Al molar ratio was measured to be 2.5, the phase could display the approximative chemical composition: γ-$Co_{0.714}Al_{0.286}OOH$. The stability of this *in situ* formed γ-$Co_{1-x}Al_xOOH$ has been proved by submitting the coated electrode to reduction at −0.1 V for over than 1000 s. The obtained diffractogram (data not shown) did not differ from that of the oxidized material, confirming the irreversibility of the oxidation process. It is noteworthy that the presence of aluminum into the LDH layers does not hamper the complete oxidation of cobalt(II) cation and the modification of the structure which seems to occur as previously described from α-$Co(OH)_2$ precursor by ozonation or in presence of NaClO [39].

EDS analysis performed on the film after the first voltammetric scan reveals no significant modification in the elemental composition of the material. In particular Co/Al atomic ratio is unchanged whereas K/Co ratio decreases to 0.5, indicating that K^+ amount is decreased with respect to the fresh film. Presence of potassium in the oxidized film may arise from a partial exchange of proton by K^+ leading to a formula derived form that proposed by Butel *et al.* [38] for γ-H_xCoO_2, i.e. γ-$H_yK_zCo_{1-x}Al_xO_2$.

The phase transformation is further confirmed by FTIR and Raman spectroscopy analysis (Fig. 4A and B, curves b). In one hand, both FTIR and Raman spectra recorded on the sample after the first cyclic voltammetry indicate the quasi-complete disappearance of the vibration bands of NO_3^- anions, confirming both the de-intercalation of this anion from the layered structure in KOH solution and the efficient dissolution of KNO_3. At low wavelength values, a prominent change is also observed. The broad $\nu_{(MOH)}$ stretching band typical of the hydroxylated brucite-like phase vanishes and the O–M–O LDH vibration bands are replaced by a strong doublet at 568 and 611 cm^{-1} on the FTIR spectrum. Vibration bands around 600 cm^{-1} corresponds to pure M(III)O_6 octahedral lattice modes.

This band appears splitted, which could be indicative of the presence of both CoO_6 and AlO_6 polyedra. Even the absorption at 3400 cm^{-1}, related to OH^- stretching appears splitted, supporting the evidence that two OH^- surroundings exist, namely Co(III)-OH and Al(III)-OH.

In another hand, vibration bands of the oxidized film observed on Raman spectra pointed at 471, 509, 608, and 673 cm^{-1} correspond to those of Co_3O_4 spinel phase according, respectively to the E_g, F_{2g} and A_{1g} modes of Co_3O_4 [40] while we were expecting vibration bands of γ-CoOOH reported to occur at 503 and 635 cm^{-1} [41]. As Raman spectra were recorded under a 10 mW laser power in order to get more intense signals, a thermal decomposition of the γ-$Co_{1-x}Al_xO(OH)$ thin film in the Co_3O_4 phase probably occurred. Such laser power effect on the γ-CoO(OH)/Co_3O_4 transformation was already reported by Pauporté *et al.* [41]. However, those results confirm the formation of a mixed Co/Al oxyhydroxide phase. The modifications observed in spectroscopy concerning both anion removal and the lattice changes are in good agreement with a structural modification of the layer induced by an increase of the oxidation state of the cobalt. Similarly, de-intercalation of chloride anions was also described during the oxidation process of α-$Co(OH)_2$ leading to γ-CoOOH [39].

In parallel, FEG-SEM image recorder after the first cycle (Fig. 2B) indicates that the film morphology is not altered by the phase oxidation and the adhesion does not seem modified. Indeed, a good adhesion of the film is still observed after cycling process.

Then, according to the PXRD analysis, it seems obvious that the irreversible mass drop observed in the EQCM experiment corresponds to the transformation of the $Co_{0.714}Al_{0.286}(OH)_2(CO_3)_{0.143}0.17\ H_2O \times KNO_3$ LDH phase into a γ-$Co_{0.714}Al_{0.286}O(OH)$ and is mainly linked to the LDH phase transformation leading to the removal of the carbonate anions from the structure. However, because of the presence of KNO_3 into the starting film and the variable amount of alkali anions which can be present into γ-CoOOH like phase, it is quite difficult to strictly quantify the mass drop.

From the second scan (Fig. 6B), the CV curves evidence two distinct oxidation and reduction peaks between 0.1 and 0.5 V associated with a small continuous and reversible mass variation. The shape of the CV is similar to that previously reported for Co/Al-LDH thin films by Wang *et al.* [16–18]. This current response has a pseudo-capacitive shape which remains unchanged for several hundreds of cycles. The number of Co moles involved in the two redox processes, calculated by integration of the peaks, is about 1×10^{-8} and therefore only 5% of the total Co cations of the starting Co/Al-LDH phase are now electroactive, thus confirming the lower electrochemical accessibility of Co cations present in the γ-CoOOH like phase generated in the first scan compared to the precursor Co/Al-LDH. The two redox processes are in good agreement with the reaction occurring during the transformation of a γ-CoOOH phase known to contain Co^{4+} centers, into a β-Co(III)OOH which can further transform in a β-$Co(OH)_2$ [38,39]. The variation of the hydrous oxide charge capacity (q_a^*), can be evaluated by integration of the total anodic current, both due to the faradic and capacitive processes, between 0.1 and 0.5 V; it depends on the square root of the scan rate ($\nu^{1/2}$) [8,42]. The total charge (q_T^*), which is proportional to the entire active layer, is obtained from extrapolation of q^* at $\nu \to 0$ on a plot q^{*-1} *vs* $\nu^{1/2}$, whereas the outer charge q_{out}^*, which is proportional to the outer active surface, is extrapolated from the q^* *vs* $\nu^{-1/2}$ plot (q^* at $\nu \to \infty$) [42]. The corresponding values are $q_T^* = 1.50 \times 10^{-4}\,C$ and $q_{out}^* = 1.03 \times 10^{-4} C$, and the difference $q_T^* - q_{out}^*$ corresponds to the charge within inner phase q_{in}^*. The ratio q_{in}^*/q_T^* is 0.3 showing that the contribution of inner sites is limited. This means that quasi-all the film thickness is involved in the pseudo-capacitive process. The corresponding specific capacitance can be evaluated from the CV of Fig. 6B, plotting the anodic current value (I_a), reported to the mass of the thin film (m), divided by <!– no-mfc –>$\nu = dV/dt(V/s)$<!– /no-mfc –>, following the formula <!– no-mfc –>$C = 2I_a dt/m$<!– /no-mfc –> dV given in units of $As/(V\,g) \approx F\,g^{-1}$ [8]. The capacitive behavior is dependent from the applied potential, but a mean value of 500 $F\,g^{-1}$ is obtained in all the investigated potential range. This value is close to that reported by Wang *et al.* [18] for Co/Al-LDH nanosheets thin films (667 $F\,g^{-1}$), thus making the material a good candidate for the development of supercapacitors devices.

4. Conclusions

Reproducible thin films of $Co_{0.714}Al_{0.86}(OH)_2(NO_3)_{0.86}{\cdot}0.6H_2O$ were prepared by electrodeposition. Two phase modifications have been highlighted during the oxidation process. In one hand, in 0.1 M KOH electrolyte an anion exchange reaction occurs leading to the formation of a carbonate intercalated Co/Al-LDH phase. In another hand, during the first oxidative scan from 0.0 to 0.6 V, an irreversible oxidation of the as-prepared Co/Al-LDH film occurs with the formation of a stable γ-$Co_{1-x}Al_xOOH$ phase. Even though only 5% of the total Co cations of the starting Co/Al-LDH phase remain electroactive after the formation of this new γ-CoOOH like phase, cyclic voltammograms have a pseudo-capacitive shape which remains unchanged for several hundreds of cycles. The corresponding specific capacitance is evaluated to 500 $F\,g^{-1}$, making the material a good candidate for the development of supercapacitors devices.

References

[1] F. Cavani, F. Trifirò, A. Vaccari, Catal. Today 11 (1991) 173.
[2] F. Trifirò, A. Vaccari, in: J.E.D. Davies, J.L. Atwood, D.D. MacNicol, F. Vgtle (Eds.), Comprehensive Supramolecular Chemistry, Pergamon Oxford, 1996, p. 251.
[3] M.R. Othman, Z. Helwani, Martunus, W.J.N. Fernando, Appl. Organomet. Chem. 23 (2009) 335.
[4] S. Kannan, Catal. Surv. Asia 10 (2006) 117.
[5] K. Takagi, T. Shichi, H. Usami, Y. Sawaki, J. Am. Chem. Soc. 115 (1993) 4339.
[6] S.J. Palmer, R.L. Frost, Ind. Eng. Chem. Res. 49 (2010) 8969.
[7] A. Malak-Polaczyk, C. Vix-Guterl, E. Frackowiak, Energy Fuels 24 (2010) 3346.
[8] T. Stimpfling, F. Leroux, Chem. Mater. 22 (2010) 974.
[9] E. Scavetta, M. Berrettoni, M. Giorgetti, D. Tonelli, Electrochim. Acta 47 (2002) 2451.
[10] E. Scavetta, D. Tonelli, Electroanalysis 14 (2002) 906.
[11] M. Morigi, E. Scavetta, M. Berrettoni, M. Giorgetti, D. Tonelli, Anal. Chim. Acta 439 (2001) 265.
[12] C. Mousty, Anal. Bioanal. Chem. 396 (2010) 315.
[13] C. Forano, S. Vial, C. Mousty, Curr. Nanosci. 2 (2006) 283.
[14] E. Scavetta, B. Ballarin, M. Berrettoni, I. Carpani, M. Giorgetti, D. Tonelli, Electrochim. Acta 51 (2006) 2129.
[15] E. Scavetta, B. Ballarin, D. Tonelli, Electroanalysis 22 (2010) 427.
[16] Y. Wang, W. Yang, C. Chen, D.G. Evans, J. Power Sources 184 (2008) 682.
[17] Y. Wang, W. Yang, S. Zhang, D.G. Evans, X. Duan, J. Electrochem. Soc. 152 (2005) A2130.
[18] Y. Wang, W. Yang, J. Yang, Electrochem. Solid State Lett. 10 (2007) A233.
[19] L.H. Su, X.-G. Zhang, J. Power Sources 172 (2007) 999.
[20] L.H. Su, X.-G. Zhang, C.H. Mi, B. Gao, Y. Liu, Phys. Chem. Chem. Phys. 11 (2009) 2195.
[21] L.H. Su, X.-G. Zhang, C.H. Mi, X.-M. Liu, J. Power Sources 179 (2008) 388.
[22] X. Guo, F. Zhang, D.G. Evans, X. Duan, Chem. Commun 46 (2010) 5197.
[23] X.-M. Liu, Y.H. Zhang, X.-G. Zhang, S.-Y. Fu, Electrochim. Acta 49 (2004) 3137.
[24] A. deRoy, C. Forano, K.E. Malki, J.P. Besse, in: M.L. Occelli, H.E. Robson (Eds.), Expanded Clays and Other Microporous Solids, Van Nostrand Reinhold, New York, 1992, p. 108.
[25] Z. Liu, R. Ma, M. Osada, N. Iyi, Y. Ebina, K. Takada, T. Sasaki, J. Am. Chem. Soc. 128 (2006) 4872.
[26] C.J. Wang, Y.A. Wu, R.M.J. Jacobs, J.H. Warner, G.R. Williams, D. O'Hare, Chem. Mater. 23 (2011) 171.
[27] J. Prince, A. Montoya, G. Ferrat, J.S. Valente, Chem. Mater. 21 (2009) 5826.
[28] T. Lopez, P. Bosch, E. Ramos, R. Gomez, O. Novaro, D. Acosta, F. Figueras, Langmuir 12 (1996) 189.
[29] V. Prevot, C. Forano, J.P. Besse, Chem. Mater. 17 (2005) 6695.
[30] E. Scavetta, A. Mignani, D. Prandstraller, D. Tonelli, Chem. Mater. 19 (2007) 4523.
[31] E. Scavetta, B. Ballarin, M. Gazzano, D. Tonelli, Electrochim. Acta 54 (2009) 1027.
[32] F. Basile, P. Benito, S. Bugani, W. De Nolf, G. Fornasari, K. Janssens, L. Morselli, E. Scavetta, D. Tonelli, A. Vaccari, Adv. Funct. Mater. 20 (2010) 4117.

[33] A. Khenifi, Z. Derriche, C. Forano, V. Prevot, C. Mousty, E. Scavetta, B. Ballarin, L. Guadagnini, D. Tonelli, Anal. Chim. Acta 654 (2009) 97.
[34] J.T. Kloprogge, R.L. Frost, Appl. Catal. 184 (1999) 61.
[35] R. Roto, L. Yu, G. Villemure, J. Electroanal. Chem. 587 (2006) 263.
[36] Z.P. Xu, H.C. Zeng, Chem. Mater. 13 (2001) 4557.
[37] Z.P. Xu, H.C. Zeng, Chem. Mater. 15 (2003) 2040.
[38] M. Butel, L. Gautier, C. Delmas, Solid State Ionics 122 (1999) 271.
[39] F. Bardé, M.-R. Palacin, B. Beaudoin, A. Delahaye-Vidal, J.-M. Tarascon, Chem. Mater. 16 (2004) 299.
[40] J. Jiang, L. Li, Mater. Lett. 61 (2007) 4894.
[41] T. Pauporte, L. Mendoza, M. Cassir, M.C. Bernard, J. Chivot, J. Electrochem. Soc. 152 (2005) C49.
[42] C.P. De Pauli, S. Trasatti, J. Electroanal. Chem. 396 (1995) 161.